Conformational transition and gelation of κ-carrageenan in electrostatic complexation with β-lactoglobulin aggregates

Hu, B., Hu, J., Han, L., Cao, J., Nishinari, K., Yang, J., Fang, Y., Li, D.

Conformational transition and gelation of κ-carrageenan in electrostatic complexation with β-lactoglobulin aggregates

Bing Hu[a], Jing Hu[b], Lingyu Han[a], Jijuan Cao[a], Katsuyoshi Nishinari[b], Jixin Yang[c], Yapeng Fang[d,*] and Dongmei Li[e]

[a]Key Lab of Biotechnology and Bioresources Utilization of Ministry of Education, College of Life Science, Dalian Minzu University, Dalian, Liaoning 116600, China;

[b]Glyn O. Phillips Hydrocolloid Research Centre at HUT, National "111" Center for Cellular Regulation and Molecular Pharmaceutics, School of Food and Biological Engineering, Hubei University of Technology, Wuhan 430068, China;

[c]Faculty of Arts, Science and Technology, Wrexham Glyndwr University, Plas Coch, Mold Road, Wrexham LL11 2AW, United Kingdom;

[d]Department of Food Science and Technology, School of Agriculture and Biology, Shanghai Jiao Tong University, Shanghai 200240, China;

[e]Collaborative Innovation Center of Seafood Deep Processing, Dalian Polytechnic University, Dalian 116034, China.

[*]Corresponding author.

Prof. Yapeng Fang

Department of Food Science and Technology, School of Agriculture and Biology, Shanghai Jiao Tong University, Shanghai 200240, China.

Email: ypfang@sjtu.edu.cn

Tel: 86-(0)-21-34208547

Abstract

The goal of this study was to evaluate the impact of electrostatic complexation with three different β-lactoglobulin aggregates on the conformational transition and gelation of κ-carrageenan (κ-car). We prepared native granular β-lactoglobulin (NGBLG), nanoparticle β-lactoglobulin (NPBLG), and fibrillary β-lactoglobulin (FBLG), and then assessed their electrostatic complexation with κ-car and the resultant impact on κ-car conformational transition, gelation, and microstructural changes. A quantitative model based on the McGhee-Hippel theory was adopted as a means of describing the impact of electrostatic complexation on the κ-car conformational transition in the presence of these protein aggregates. FBLG resulted in the most significant inhibition of κ-car conformational transition and gelation, whereas NPBLG had the least significant impact on this process. This was attributed to the fact that NPBLG imposed the least steric hindrance of these three aggregates. Together, these data highlight promising approaches to regulating polysaccharide gelation, viscoelasticity, rheological behavior, and conformational transition for use in a range of industrial applications.

Keywords: conformational transition, gelation, electrostatic complexation, aggregates

1. Introduction

Protein/polyelectrolyte electrostatic complexation is a key process that is commonly leveraged for the design of food products that are low in calorie and starch content (Wu, Degner, & McClements, 2014), the encapsulation of flavors and probiotics (Bosnea, Moschakis, & Biliaderis, 2014; Yeo, Bellas, Firestone, Langer, & Kohane, 2005), and the stabilization of emulsions and foams (Li, Fang, Al-Assaf, Phillips, & Jiang, 2012). Such complexation is also utilized in biotechnological and pharmaceutical applications including protein separation and purification (Du, Dubin, Hoagland, & Sun, 2014), enzyme stabilization and immobilization (Kayitmazer, Seeman, Minsky, Dubin, & Xu, 2013), drug delivery (Saravanan & Rao, 2010), and gene therapy (Elzoghby, Samy, & Elgindy, 2012). Natural polyelectrolytes can adopt a range of different conformations when in solution, including aggregates, random coils, spherical structures, and single/multiple spiral structures (Choi & Majima, 2011; Tanrikulu, Forticaux, Jin, & Raines, 2016; Tao, Zhang, Yan, & Wu, 2007). These conformations are associated with a range of biological processes (Choi & Majima, 2011) and human diseases (Ye et al., 2012), and determine the bioactive properties of these polyelectrolytes (Chen, Xu, Zhang, & Zeng, 2009). Protein/polyelectrolyte electrostatic coordination and conformational transformation are commonly observed in specific technical applications and in the context of certain biological processes. Prior work has shown that the interrelated processes of chain stiffening and specific ion binding ultimately influence polyelectrolyte conformational transitions and thereby impact protein/polyelectrolyte complexes. (Cao, Fang, Nishinari, & Phillips, 2016). In industrial contexts, polyelectrolyte conformational transition has been leveraged for thickening, stabilizing, and gelling applications.

κ-carrageenan (κ-car) is a sulfated D-galactan polysaccharide composed of repeating disaccharide alternating (1→3) β−D-galactose-4-sulfate and (1→4) α-3,6-anhydro-D-galactose units. Owing to its ability to facilitate the formation of hard and brittle gels, κ-car is commonly utilized as a gelling agent and stabilizer in the food industry, exhibiting both syneresis and thermal hysteresis. When hot κ-car solutions are cooled, gelation occurs through a process which involves a coil-helix transition and subsequent spiral aggregation (De Ruiter & Rudolph, 1997). While the details pertaining to κ-car conformal transformation remain controversial (Djabourov, Nishinari, & Ross-Murphy, 2013), it is thought to undergo a transition from a random coil structure to a double helix structure in the presence of specific ions (such as K^+), with helix aggregation occurring as temperatures are reduced (Grasdalen & Smidsroed, 1981). This coil-to-double helix transition is an essential step in the gelling process. Altering local levels of particular cations (including K^+, Cs^+, and Rb^+) has been shown to increase double helix stability, thereby facilitating helix-helix aggregation and consequent gelation. Ultimately, double helix aggregation occurs in a manner that is dependent upon both cation type and concentrations at a given critical temperature (Rochas & Rinaudo, 1984).

Milk-derived natural globular β-lactoglobulin (NGBLG) is a spherical protein found in high levels in whey that has been the subject of significant research interest owing to its nutritional and functional properties (Simons, Mcclenaghan, & Clark, 1987). NGBLG adopts a compact globular structure, and is composed of 162 amino acid residues, one thio group, and two disulfide bonds (molecular mass = 18.3 kDa) (Chen et al., 2006; Papiz et al., 1986). β-lactoglobulin has been shown by Bromely et al. (2004) to have an isoelectric point in the pH 4.7–5.2 range, wherein protein degeneration occurs and the natural conformation can be

disrupted upon exposure to heat or pressure (Manderson, Hardman, & Creamer, 1998; Roefs & De Kruif, 1994). By heating NGBLG above its denaturation temperature results in the partial unwinding of its globular structure and the exposure of previously buried groups, after which hydrogen bonding and hydrophobic interactions can result in different forms of molecular aggregation. While such aggregation is often irreversible, it is ultimately dependent on the formation of disulfide bonds between cysteine residues within the NGBLG polypeptide chain (Nicolai, Britten, & Schmitt, 2011). Adjusting the pH of an aqueous solution containing NGBLG can drive this protein to form amyloid fibrils or nanoparticles owing to its unique associative processes (Gottschalk, Nilsson, Roos, & Halle, 2003). For example, heating whey proteins at 80°C and pH 2.0 for several hours results in protein hydrolysis, with some of the resultant peptides undergoing fibril self-assembly (van der Linden & Venema, 2007). Mehalebi, Nicolai, & Durand (2008) previously characterized the concentration-dependent aggregation of these proteins at different pH values (5.8, 6.0, 6.5, 7.0, and 8.0), and found that weak hydrogen bonding interactions between monomers and the conversion of intramolecular β-sheets to intermolecular β-sheets resulted in the formation of large aggregates, the sizes of which rose with increasing protein concentration (Kavanagh, Clark, & Ross-Murphy, 2000). Food protein-based nanoparticles have also been the subject of extensive research interest owing to their biocompatibility and advantageous properties (Etorki, Gao, Sadeghi, Maldonado-Mejia, & Kokini, 2016).

In previous studies, it has been clarified that the conformational transition of κ-car is affected and tuned by electrostatic complexation with native granular β-lactoglobulin (Cao et al., 2016). Different conditions in food processing lead to different aggregates of protein by

adjusting pH and temperature (Hu et al., 2019). However, to the best of our knowledge, no direct and systematic comparison has been made so far on the conformational transition and gelation of natural polyelectrolytes influenced by electrostatic complexation with native, nanoparticulate and fibrillar proteins. The goal of the present study was to understand how the conformational transition and gelation of κ-car was impacted by electrostatic complexation with native granular β-lactoglobulin and aggregates thereof (nanoparticle β-lactoglobulin and fibrillar β-lactoglobulin). The resultant data will advance the current understanding of protein/polyelectrolyte electrostatic complexation behavior, thereby facilitating the development of more complex systems.

2. Materials and methods

2.1 Materials

NGBLG was obtained from milk as detailed previously by Toro-Sierra, Tolkach, & Kulozik (2013). κ-car was obtained from FMC biopolymer (Gelcarin GP-911NF) in the form of a sodium salt via ion-exchange resin (Amberlite IR-120, Sigma), after which it was freeze-dried. Atomic absorption spectrometry revealed that the lyophilized κ-car powder contained 6.32% Na, 0.067% K, 0.0027% Mg, and 0.0083% Ca. This powder had the following molecular parameters, as determined via GPC-MALLS at 25°C in 0.1 M NaI with a Shodex OHpak SB-805 separation column (GE Healthcare Co., USA): M_w = 467 kD*a*; M_w/M_n = 1.2; R_g = 85.0 nm. This analysis indicated a double-helical κ-car conformation without any further aggregation. Ultrapure (18.25 MΩ.cm) water was prepared with a Milli-Q system.

2.2 Nanoparticle β-lactoglobulin (NPBLG) and fibrillar β-lactoglobulin (FBLG)

127 ***preparation***

128 NPBLGs and FBLGs were prepared as previously described by Hu et al. (2019).
129 **Preparation of NPBLGs:** NGBLG solution (10 mg/mL) of pH 5.8 was heated in an 85 °C
130 water bath for 15 min and cooled in ice water for 20 min. The solution was dialyzed against
131 pH 5.8 water at 4 °C for 72 h (MWCO = 50 kDa, Biosharp). Finally, the sample was freeze-
132 dried to obtain NPBLG. **Preparation of FBLGs:** NGBLG solution (20 mg/mL) of pH 2.0 was
133 heated in an 80 °C water bath for 16 h and cooled in ice water for 20 min. The solution was
134 dialyzed against pH 2.0 water at 4 °C for 72 h (MWCO = 100 kDa, Biosharp). Finally, the
135 sample was freeze-dried to obtain FBLG.

136 ***2.3 Mixture Solution Preparation***

137 Stock solutions of 0.18−1.80 wt % NGBLG and NPBLG, 0.09−0.72 wt % FBLG and
138 0.90 wt % κ-car were prepared by dissolving appropriate amounts of samples into 50 mM KCl.
139 κ-car solutions were heated at 85 °C for 1 h under magnetic stirring. NGBLG, NPBLG and
140 FBLG solutions were dissolved at ambient temperature overnight on a roller mixer. NGBLG,
141 NPBLG and FBLG/κ-car mixtures at a fixed κ-car concentration (0.15 wt %) and various
142 mixing ratios (NGBLG and NPBLG w/w, $0 < r < 10$; FBLG w/w, $0 < r < 4$ (when $r>4$, the
143 FBLG completely inhibited the gelling behavior of κ-car)) were prepared by blending the stock
144 solutions, followed by stirring at 60 °C for 10 min. The mixing temperature was chosen to
145 avoid the denaturation of NGBLG and its aggregates at high temperature and meanwhile ensure
146 a sol state of κ-car. pH of the mixtures was adjusted to targeted values using 2 M NaOH or HCl.
147 In our previous investigation, the isoelectric points (IEPs) of NGBLG, NPBLG and FBLG were
148 4.9, 4.7 and 4.64, respectively. The zeta potential of κ-car, measured in the pH range of 2−9, is

characteristic of strong polyelectrolytes with nearly a constant value of about −50 mV (Hu et al., 2019). Therefore, two representative pHs (pH=9.0 and pH=4.0) were selected to evaluate the impact of electrostatic complexation with NGBLG and its aggregates on the conformational transition and gelation of κ-car.

2.4 Rheological measurements

The rheological properties of κ-car, NGBLG/κ-car, NPBLG/κ-car, and FBLG/κ-car mixtures were evaluated with a rotational Haake Rheostress 6000 rheometer (Thermo Fisher Scientific, USA) and a serrated parallel-plate geometry (diameter 35 mm; gap 1.0 mm) as previously detailed by Cao et al. (2016).

2.5 Differential scanning calorimetry (DSC)

κ-car thermal properties during cooling from 60 ºC to 0ºC in different NGBLG/κ-car, NPBLG/κ-car, and FBLG/κ-car mixtures were assessed with a high-sensitivity microcalorimeter DSC III (Setaram, France) as previously detailed by Cao et al. (2016).

2.6 Atomic force microscopy (AFM) imaging

AFM measurements of κ-car or NGBLG/κ-car, NPBLG/κ-car and FBLG/κ-car mixtures were conducted with a MultiMode 8 Scanning Probe Microscope (Bruker, USA) as described previously (Hu et al., 2019).

3. Results and discussion

We began by preparing a series of NGBLG aggregates with differing particle sizes via adjusting pH and temperature values, as described previously (Hu et al., 2019). Proteins can

form electrostatic complexes with anionic polyelectrolytes at pH values that are below or slightly above the corresponding isoelectric point values (Weinbreck, de Vries, Schrooyen, & De Kruif, 2003). As such, we evaluated NGBLG/κ-car, NPBLG/κ-car, and FBLG/κ-car mixtures at a range of pH values (pH = 9.0 and 4.0) and mixing ratios to assess the impact of electrostatic complexation on conformational transition (Fig. 1). At high temperatures, κ-car exhibits a random coil conformation. We detected a sharp increase in the storage modulus (G') at 40.6 °C for 0.15% (w/w) κ-car when cooling at pH 9.0 (Fig. 1A-C) as a consequence of gelation (Madbouly & Otaigbe, 2005), indicating that combining κ-car with NGBLG or aggregates thereof at a pH of 9.0 does not impact the temperature at which gelation is initiated. In contrast, the G' values for 0.15% (w/w) κ-car solutions mixed with NGBLG, NPBLG, and FBLG reduced significantly with increasing mixing ratio (r) at pH 4.0 (Fig. 1D-F). As such, κ-car gelation was completely disrupted for FBLG, NGBLG, and NPBLG mixtures at respective r values of 3.0, 4.0, and 6.0 at this pH. We also observed the frequency dependence of κ-car gel viscoelasticity for the tested NGBLG, NPBLG, and FBLG mixtures at 10°C in different ratios (Fig. 1A-F). At a pH of 9.0, these solutions exhibited typical elastic gel characteristics with moduli being independent of frequency and G'>G", indicating that NGBLG or its aggregates had no impact on gelation and gel viscoelasticity at this pH. In contrast, at a pH of 4.0 G' and G" became increasingly frequency-dependent with rising r-value, consistent with a weak viscoelastic gel or viscous solution (Derkach, Ilyin, Maklakova, Kulichikhin, & Malkin, 2015). We have previously reported on the relationship between Zeta potential (ζ) and pH for NGBLG, NPBLG, and FBLG (Hu et al., 2019). At pH 9.0, NGBLG/κ-car, NPBLG/κ-car, and FBLG/κ-car mixtures exhibit no electrostatic complexation as all of these compounds are negatively

charged. In contrast, at pH 4.0, κ-car and NGBLAG or aggregates thereof exhibit opposite charges, resulting in strong electrostatic complexation within the NGBLG/κ-car, NPBLG/κ-car, and FBLG/κ-car mixtures, respectively. These results suggest that mixing κ-car mixed with protein or protein aggregate solutions in particular conditions can result in electrostatic complexation and thereby alter polyelectrolyte gelling behavior, yielding solutions with viscoelastic properties that range from elastic gels to viscous solutions.

Figure 2 demonstrates the impact of NGBLG or its aggregates on the conformational transition of κ-car, revealing that electrostatic complexation with NGBLG or its aggregates was sufficient to influence κ-car gelation. We assessed the storage modulus (G′) gelation profiles for κ-car at different NGBLG, NPBLG, FBLG/κ-car mixing ratios (r) at 30°C. At a pH of 9.0, there were almost no changes in the gelling ability or viscoelasticity of κ-car complexed with NGBLG, NPBLG, FBLG (Fig. 2A). In contrast, at a pH of 4.0, G′ and G″ declined with the rising presence of NGBLG or aggregates thereof, suggesting that the gelling ability and viscoelasticity of κ-car was greatly reduced at this pH. These findings suggested that NGBLG and its aggregates can modulate the properties of κ-car gels, with FBLG having the most robust suppressive effect on κ-car conformational transition, followed by NGBLG and NPBLG.

Next, we analyzed DSC peaks for NGBLG/κ-car, NPBLG/κ-car, and FBLG/κ-car mixtures during cooling in different ratios at pH 9.0. The DSC curve for pure κ-car exhibited an asymmetric exothermic peak with an initial temperature of 40.7 °C, consistent with the coil-helix transition of κ-car (Cao et al., 2016). With a similar initial temperature of about 40°C, the exothermic peak changed slightly with increasing NGBLG/κ-car, NPBLG/κ-car and FBLG/κ-car mixing ratios (r) (NGBLG from 0 - 10, NPBLG from 0 - 10, FBLG from 0 - 4), and the

enthalpy change (ΔH) was approximately 50 mJ/g (Fig. 3A-C). At pH 9.0, the conformational transition of κ-car during cooling was largely unaffected by mixing with NGBLG or aggregates thereof, as there was no electrostatic complexation between κ-car and NGBLG or its aggregates at this pH, which was above the isoelectric point such that these compounds were all negatively charged (Weinbreck et al., 2003). In contrast, at a pH of 4.0, which was below the IEP, increasing the mixing ratios for NGBLG or its aggregates significantly decreased the exothermic peak associated with the κ-car coil-to-helix transition (Fig. 3D-F). The exothermic peak of FBLG/κ-car, NGBLG/κ-car, and NPBLG/κ-car tended to disappear completely at r values over 3, 4, and 6, respectively. The decreases in denaturation temperature indicate that NGBLG and its aggregates exhibited reduced conformational or tertiary structural stability following electrostatic complexation with κ-car. Overall, these data indicated that at a pH of 4.0, mixing κ-car with NGBLG or its aggregates significantly suppressed its conformational transformation. This is attributable to the electrostatic complexation between NGBLG/κ-car, NPBLG/κ-car, or FBLG/κ-car, which disrupted κ-car helix formation. With respect to their relative ability to suppress κ-car conformational transformation, FBLG exhibited maximal suppression, followed by NGBLG and NPBLG, in line with our above results. We further found that the ΔH of the κ-car conformational transition of changed as a function of mixing ratio at pH 4.0 (Fig. 3D-F). We observed a two-step reduction of ΔH associated with the electrostatic complexation between NGBLG/κ-car, NPBLG/κ-car or FBLG/κ-car with increasing mixing ratios occurring at r = 0.31, 0.95, and 0.81, respectively. Above these r values, the decrease in ΔH clearly accelerated, indicating the more significant disruption of κ-car conformational transition at these ratios. The transition from soluble to insoluble electrostatic complexes has

been shown to result in a sudden ΔH decrease at the turning point (Mekhloufi, Sanchez, Renard, Guillemin, & Hardy, 2005; Weinbreck et al., 2003). We have previously found that above the critical pH, electrostatic complexation can occur effectively, and a model of structural transitions between regions has been proposed (Fang, Li, Inoue, Lundin, & Appelqvist, 2006; Li et al., 2012).

We additionally evaluated κ-car gel microstructures for NGBLG/κ-car, NPBLG/κ-car, and FBLG/κ-car mixtures at a fixed mixing ratio (r = 3) and pH 4.0 (Fig. 4). While unmodified κ-car gel exhibited a double helix structure with a three-dimensional network that formed as a result of aggregation during cooling, this double helix structure was absent for the NGBLG/κ-car and FBLG/κ-car mixtures and was significantly attenuated for the NPBLG/κ-car mixture. This further confirmed that electrostatic complexation with different NGBLG aggregates suppressed the κ-car coil-to-helix transition, with NGBLG and FBLG exhibiting a more robust suppressive effect relative to NPBLG. This suggested that the NGBLG aggregation state can impact κ-car conformational transition.

As shown above, at pH 4.0, the electrostatic complexation of κ-car with NGBLG or its aggregates markedly suppresses the corresponding conformational transition, as NGBLG or its aggregates physically occupy the surface/structure of κ-car. The relative degree of κ-car conformational transition is thus likely associated with the number of repetitive units unoccupied by these NGBLB aggregates. By utilizing the DNA-protein binding theory posited by McGhee-Hippel, we were able to develop a quantitative model describing the impact of the electrostatic complexation of NGBLG/κ-car, NPBLG/κ-car, and FBLG/κ-car mixtures on polyelectrolyte conformational transition (McGhee & von Hippel, 1974):

$$\left(1-\emptyset(\mathrm{r})\right)\left[\emptyset(r)+\frac{1-\emptyset(r)}{m}\right]^{m-1}-Km\emptyset(r)^{m}\left[r\frac{\mathrm{C}_{p}M_{w}^{P}}{M_{w}^{Pr}}-\mathrm{C}_{p}\frac{N(1-\emptyset(r))}{m}\right]=0 \quad (1)$$

where r corresponds to the protein/polyelectrolyte mixing ratio; $\emptyset(\mathrm{r})$ corresponds to the relative degree of polyelectrolyte conformational transition; m is the number of consecutive repeating polyelectrolyte units covered by protein molecules and is the reciprocal of the binding stoichiometry (n); *K* represents the binding constant; C_{p} corresponds to the polyelectrolyte molar concentration; M_{w}^{p} and M_{w}^{Pr} indicate respective polyelectrolyte and protein molecular weights; and *N* represents the number of repeating polyelectrolyte units. We have previously utilized the McGhee-Hippel approach successfully to assess the impact of NGBLG hydrolysates on κ-car gelation (Cao, Li, Fang, Nishinari, & Phillips, 2016). However, in the present study, we assessed the conformational effect rather than the effect on molar mass.

Next, ∅, which was measured via DSC, was assessed as a function of NGBLG/κ-car, NPBLG/κ-car, and FBLG/κ-car mixing ratio at pH 4.0 (above the IEP of NGBLG or its aggregates) (Fig. 5). The resultant solid lines were a satisfactory match to Equation one when using the following calculation parameters for this experimental system: N=572, C_{p} =6.42×10^{-6} mol/L, M_{w}^{Pr} =1.91×10^{4} Da, and M_{w}^{p} =2.34×10^{5} Da. The calculated thermodynamic binding parameters (m and K) at the tested pH are shown in Table 1. Based on the consistency between our model and Equation 1, we concluded that we were able to experimentally measure $\emptyset(\mathrm{r})$ as the ratio of the enthalpy change of the conformational transition of NGBLG/κ-car, NPBLG/κ-car, and FBLG/κ-car mixtures (ΔH(r)) to that of pure κ-car (ΔH(r = 0)). All tested mixtures exhibited significant decreases with increasing r values, which may indicate that the insoluble NGBLG/κ-car, NPBLG/κ-car, and FBLG/κ-car began to form complexes, whereas the conformational transition of NGBLG/κ-car, NPBLG/κ-car, and

FBLG/κ-car was significantly inhibited. The binding constant (K) values for NGBLG/κ-car, NPBLG/κ-car and FBLG/κ-car electrostatic complexation mixtures were 3.1×10^8, 5×10^7, and 5×10^{10}, respectively. The changes in K were attributable to the changes in the electrostatic attraction of NGBLG or its aggregates. There were 12.5, 9.5, and 20.5 consecutive repeating units covered by a single protein molecule (m) in respective NGBLG/κ-car, NPBLG/κ-car, and FBLG/κ-car electrostatic complexation mixtures. Based on the length of one κ-car repeating unit (1.03 nm) (Vreeman, Snoeren, & Payens, 1980), the m value of NGBLG/κ-car mixture was 12.5, consistent with a 12.9 nm consecutive binding length, in line with the β-lg diameter (2Rg = 13 nm) measured via GPC-MALLS. In contrast, at a pH of 4.0, the m values of NPBLG/κ-car and FBLG/κ-car electrostatic complexation mixtures were 9.5 and 20.5, respectively, matching the consecutive binding lengths of 9.8 and 21.1 nm. One possible explanation is that the alteration in length was the result of changes in protein surface charge and aggregation state, thus increasing its effective Debye length.

A schematic overview of the putative impact of electrostatic complexation with NGBLG or aggregates thereof on κ-car conformational transition during cooling is shown in Figure 6. Under acidic conditions, NPBLG and FBLG can be prepared via nucleated aggregation (Jansens et al., 2019). Monomeric proteins or peptide derivatives thereof can merge to generate oligomers, which can then undergo self-assembly to yield fibers and nanoparticles (Adamcik & Mezzenga, 2011; Hill, Robinson, Matthews, & Muschol, 2009). As many positively charged groups are sequestered within spherical nanoparticles, the efficiency of NPBLG/κ-car electrostatic complexation was somewhat reduced (Table 1). As such, κ-car exhibits sufficient freedom to adopt a helical conformation in this context. At a low mixing ratio, κ-car

303 conformational transition is disrupted via electrostatic complexation with NPBLG. In contrast,
304 in NGBLG/κ-car and FBLG/κ-car electrostatic complexation mixtures, κ-car molecules were
305 sterically blocked and were thus unable to efficiently form helical structures owing to the
306 extensive binding of these κ-car molecules to NGBLG or FBLG. As such, the conformational
307 transition of κ-car was markedly inhibited following electrostatic complexing with NGBLG or
308 FBLG.
309
310 **4. Conclusions**
311 Herein, we studied the conformational transition and gelation of κ-car following
312 electrostatic complexation with NGBLG or aggregates thereof, revealing significant
313 differences in NGBLG/κ-car, NPBLG/κ-car, and FBLG/κ-car conformational transition and
314 gelation properties. This effect was closely linked to the NGBLG aggregation state at low pH
315 values. In contrast, GBLG was able to more effectively inhibit the κ-car conformational
316 transition owing to the high degree of associated physical hindrance, whereas NPBLG was a
317 weak inhibitor of this process. We successfully developed a quantitative model of these results
318 based on the McGhee-Hippel theory, and we used this model to describe the impact of protein
319 and protein aggregate electrostatic complexation on polyelectrolyte conformational transition.
320 Overall, our data highlight promising approaches to controlling the gelation and related
321 properties of polyelectrolytes through electrostatic complexation with specific proteins or
322 aggregates thereof.
323
324

Acknowledgments

This work was supported by National Natural Science Foundation of China (No. 31671811 and No. 31701555), the State Key Research and Development Plan "Modern Food Processing and Food Storage and Transportation Technology and Equipment" (No. 2017YFD0400200), Dalian Science and Technology Innovation Foundation (No. 2020JJ26SN059) and the grant from Shanghai Science and Technology Committee (No. 18JC1410801).

CRediT authorship contribution statement

Yapeng Fang: Conceptualization, Methodology. **Bing Hu:** Data curation, Software, Writing Original draft preparation. **Jing Hu and Lingyu Han:** Visualization, Investigation. **Jijuan Cao and Katsuyoshi Nishinari:** Supervision. **Dongmei Li:** Software, Validation. **JixinYang:** Writing- Reviewing and Editing.

References

Adamcik, J., & Mezzenga, R. (2011). Proteins fibrils from a polymer physics perspective. *Macromolecules*, *45*(3), 1137-1150. https://doi.org/10.1021/ma202157h.

Bosnea, L. A., Moschakis, T., & Biliaderis, C. G. (2014). Complex coacervation as a novel microencapsulation technique to improve viability of probiotics under different stresses. *Food and Bioprocess Technology*, *7*(10), 2767-2781. https://doi.org/10.1007/s11947-014-1317-7.

Bromley, E. H. C., Krebs, M. R. H., & Donald, A. M. (2004). Aggregation across the length-scales in β-lactoglobulin. *Faraday Discussions*, *128*(2), 13-27. https://doi.org/10.1039/B403014A.

Cao, Y., Fang, Y., Nishinari, K., & Phillips, G. O. (2016). Effects of conformational ordering on protein/polyelectrolyte electrostatic complexation: ionic binding and chain stiffening. *Scientific Reports*, *6*(1), 23739. https://doi.org/10.1038/srep23739.

Cao, Y., Li, S., Fang, Y., Nishinari, K. & Phillips, G. O. (2016). Conformational transition of polyelectrolyte as influenced by electrostatic complexation with protein. *Biomacromolecules*, *17*(12), 3949-3956. https://doi.org/10.1021/acs.biomac.6b01335.

354 Chen, W. L., Liu, W. T., Yang, M. C., Hwang, M. T., Tsao, J. H., & Mao, S. J. T. (2006). A
355 novel conformation-dependent monoclonal antibody specific to the native structure of β-
356 lactoglobulin and its application. *Journal of Dairy Science*, *89*(3), 912-921.
357 https://doi.org/10.3168/jds.S0022-0302(06)72156-7.
358 Chen, X., Xu, X., Zhang, L., & Zeng, F. (2009). Chain conformation and anti-tumor activities
359 of phosphorylated (1→3)-β-D-glucan from Poria cocos. *Carbohydrate Polymers*, *78*(3),
360 581-587. https://doi.org/10.1016/j.carbpol.2009.05.019.
361 Choi, J., & Majima, T. (2011). Conformational changes of non-B DNA. *Chemical Society*
362 *Reviews*, *40*(12), 5893-5909. https://doi.org/10.1039/C1CS15153C.
363 De Ruiter, G. A., & Rudolph, B. (1997). Carrageenan biotechnology. *Trends in Food Science*
364 *& Technology*, *8*(12), 389-395.
365 Derkach, S. R., Ilyin, S. O., Maklakova, A. A., Kulichikhin, V. G., & Malkin, A. Y. (2015). The
366 rheology of gelatin hydrogels modified by κ-carrageenan. *LWT - Food Science and*
367 *Technology*, *63*(1), 612-619. https://doi.org/10.1016/j.lwt.2015.03.024.
368 Djabourov, M., Nishinari, K. & Ross-Murphy, S. B. (2013). *Physical gels from biological and*
369 *synthetic polymers*. UK: Cambridge University Press.
370 Du, X. S., Dubin, P. L., Hoagland, D. A., & Sun, L. H. (2014). Protein-selective coacervation
371 with hyaluronic acid. *Biomacromolecules*, *15*(3), 726-734.
372 https://doi.org/10.1021/bm500041a.
373 Elzoghby, A. O., Samy, W. M., & Elgindy, N. A. (2012). Protein-based nanocarriers as
374 promising drug and gene delivery systems. *Journal of Controlled Release*, *161*(1), 38-49.
375 https://doi.org/10.1016/j.jconrel.2012.04.036.

376 Etorki, A. M., Gao, M., Sadeghi, R., Maldonado-Mejia, L. F., & Kokini, J. L. (2016). Effects
377 of desolvating agent types, ratios, and temperature on size and nanostructure of
378 nanoparticles from α-lactalbumin and ovalbumin. *Journal of Food Science*, *81*(10), E2511-
379 E2520. https://doi.org/10.1111/1750-3841.13447.
380 Fang, Y., Li, L., Inoue, C., Lundin, L., & Appelqvist, I. (2006). Associative and segregative
381 phase separations of gelatin/κ-carrageenan aqueous mixtures. *Langmuir*, *22*(23), 9532-
382 9537. https://doi.org/10.1021/la061865e.
383 Gottschalk, M., Nilsson, H., Roos, H., & Halle, B. (2003). Protein self-association in solution:
384 The bovine β-lactoglobulin dimer and octamer. *Protein Science*, *12*(11), 2404-2411.
385 https://doi.org/10.1110/ps.0305903.
386 Grasdalen, H., & Smidsroed, O. (1981). Iodide-specific formation of .kappa.-carrageenan
387 single helixes. Iodine127 NMR spectroscopic evidence for selective site binding of iodide
388 anions in the ordered conformation. *Macromolecules*, *14*(6), 1842-1845.
389 Hill, S. E., Robinson, J., Matthews, G., & Muschol, M. (2009). Amyloid protofibrils of
390 lysozyme nucleate and grow via oligomer fusion. *Biophysical Journal*, *96*(9), 3781-3790.
391 https://doi.org/10.1016/j.bpj.2009.01.044.
392 Hu, J., Yang, J., Xu, Y., Zhang, K., Nishinari, K., Phillips, G. O., & Fang, Y. (2019).
393 Comparative study on foaming and emulsifying properties of different beta-lactoglobulin
394 aggregates. *Food & Function*, *10*(9), 5922-5930. https://doi.org/10.1039/C9FO00940J.
395 Jansens, K. J. A., Rombouts, I., Grootaert, C., Brijs, K., Van Camp, J., Van der Meeren, P.,
396 Rousseau, F., Schymkowitz, J., & Delcour, J. A. (2019). Rational design of amyloid-like
397 fibrillary structures for tailoring food protein techno-functionality and their potential health

implications. *Comprehensive Reviews in Food Science and Food Safety*, *18*(1), 84-105. https://doi.org/10.1111/1541-4337.12404.

Kavanagh, G. M., Clark, A. H., & Ross-Murphy, S. B. (2000). Heat-induced gelation of globular proteins: part 3. Molecular studies on low pH beta-lactoglobulin gels. *International Journal of Biological Macromolecules*, *28*(1), 41-50. https://doi.org/10.1016/S0141-8130(00)00144-6.

Kayitmazer, A. B., Seeman, D., Minsky, B. B., Dubin, P. L., & Xu, Y. S. (2013). Protein-polyelectrolyte interactions. *Soft Matter*, *9*(9), 2553-2583. https://doi.org/10.1039/C2SM27002A.

Li, X., Fang, Y., Al-Assaf, S., Phillips, G. O., & Jiang, F. (2012). Complexation of bovine serum albumin and sugar beet pectin: Stabilising oil-in-water emulsions. *Journal of Colloid and Interface Science*, *388*(1), 103-111. https://doi.org/10.1016/j.jcis.2012.08.018.

Li, X., Fang, Y., Al-Assaf, S., Phillips, G. O., Yao, X., Zhang, Y., Zhao, M., Zhang, K., & Jiang, F. (2012). Complexation of bovine serum albumin and sugar beet pectin: Structural transitions and phase diagram. *Langmuir*, *28*(27), 10164-10176. https://doi.org/10.1021/la302063u.

Madbouly, S. A., & Otaigbe, J. U. (2005). Rheokinetics of thermal-induced gelation of waterborne polyurethane dispersions. *Macromolecules*, *38*(24), 10178-10184. https://doi.org/10.1021/ma0511088.

Manderson, G. A., Hardman, M. J., & Creamer, L. K. (1998). Effect of heat treatment on the conformation and aggregation of β-lactoglobulin A, B, and C. *Journal of Agricultural & Food Chemistry*, *46*(12), 5052-5061. https://doi.org/10.1021/jf980515y.

McGhee, J. D., & von Hippel, P. H. (1974). Theoretical aspects of DNA-protein interactions: Co-operative and non-co-operative binding of large ligands to a one-dimensional homogeneous lattice. *Journal of Molecular Biology*, *86*(2), 469-489. https://doi.org/10.1016/0022-2836(74)90031-X.

Mehalebi, S., Nicolai, T., & Durand, D. (2008). Light scattering study of heat-denatured globular protein aggregates. *International Journal of Biological Macromolecules*, *43*(2), 129-135. https://doi.org/10.1016/j.ijbiomac.2008.04.002.

Mekhloufi, G., Sanchez, C., Renard, D., Guillemin, S., & Hardy, J. (2005). pH-induced structural transitions during complexation and coacervation of β-lactoglobulin and acacia gum. *Langmuir*, *21*(1), 386-394. https://doi.org/10.1021/la0486786.

Nicolai, T., Britten, M., & Schmitt, C. (2011). β-Lactoglobulin and WPI aggregates: Formation, structure and applications. *Food Hydrocolloids*, *25*(8), 1945-1962. https://doi.org/10.1016/j.foodhyd.2011.02.006.

Papiz, M. Z., Sawyer, L., Eliopoulos, E. E., North, A. C. T., Findlay, J. B. C., Sivaprasadarao, R., Jones, T. A., Newcomer, M. E., & Kraulis, P. J. (1986). The structure of β-lactoglobulin and its similarity to plasma retinol-binding protein. *Nature*, *324*(6095), 383-385. https://doi.org/10.1038/324383a0.

Rochas, C., & Rinaudo, M. (1984). Mechanism of gel formation in κ-carrageenan. *Biopolymers*, *23*(4), 735-745. https://doi.org/10.1002/bip.360230412.

Roefs, S. P., & De Kruif, K. G. (1994). A model for the denaturation and aggregation of β-lactoglobulin. *European Journal of Biochemistry*, *226*(3), 883-889. https://doi.org/10.1111/j.1432-1033.1994.00883.x.

Saravanan, M., & Rao, K. P. (2010). Pectin-gelatin and alginate-gelatin complex coacervation for controlled drug delivery: Influence of anionic polysaccharides and drugs being encapsulated on physicochemical properties of microcapsules. *Carbohydrate Polymers*, *80*(3), 808-816. https://doi.org/10.1016/j.carbpol.2009.12.036.

Simons, J. P., Mcclenaghan, M., & Clark, A. J. (1987). Alteration of the quality of milk by expression of sheep β-lactoglobulin in transgenic mice. *Nature*, *328*(6130), 530-532.

Tanrikulu, I. C., Forticaux, A., Jin, S., & Raines, R. T. (2016). Peptide tessellation yields micrometre-scale collagen triple helices. *Nature Chemistry*, *8*(11), 1008-1014. https://doi.org/10.1038/nchem.2556.

Tao, Y., Zhang, L., Yan, F., & Wu, X. (2007). Chain conformation of water-insoluble hyperbranched polysaccharide from fungus. *Biomacromolecules*, *8*(7), 2321-2328. https://doi.org/10.1021/bm070335+.

Toro-Sierra, J., Tolkach, A., & Kulozik, U. (2013). Fractionation of α-lactalbumin and β-lactoglobulin from whey protein isolate using selective thermal aggregation, an optimized membrane separation procedure and resolubilization techniques at pilot plant scale. *Food & Bioprocess Technology*, *6*(4), 1032-1043. https://doi.org/10.1007/s11947-011-0732-2.

van der Linden, E., & Venema, P. (2007). Self-assembly and aggregation of proteins. *Current Opinion in Colloid & Interface Science*, *12*(4-5), 158-165. https://doi.org/10.1016/j.cocis.2007.07.010.

Vreeman, H. J., Snoeren, T. H. M., & Payens, T. A. J. (1980). Physicochemical investigation of *k*-carrageenan in the random state. *Biopolymers*, *19*(7), 1357-1374. https://doi.org/10.1002/bip.1980.360190711.

Weinbreck, F., de Vries, R., Schrooyen, P., & De Kruif, C. G. (2003). Complex coacervation of whey proteins and gum arabic. *Biomacromolecules*, *4*(2), 293-303. https://doi.org/10.1021/bm025667n.

Wu, B. C., Degner, B., & McClements, D. J. (2014). Soft matter strategies for controlling food texture: formation of hydrogel particles by biopolymer complex coacervation. *Journal of Physics: Condensed Matter*, *26*(46), 464104. https://doi.org/10.1088/0953-8984/26/46/464104.

Ye, Y., Blaser, G., Horrocks, M. H., Ruedas-Rama, M. J., Ibrahim, S., Zhukov, A. A., Orte, A., Klenerman, D., Jackson, S. E., & Komander, D. (2012). Ubiquitin chain conformation regulates recognition and activity of interacting proteins. *Nature*, *492*(7428), 266-270. https://doi.org/10.1038/nature11722.

Yeo, Y., Bellas, E., Firestone, W., Langer, R., & Kohane, D. S. (2005). Complex coacervates for thermally sensitive controlled release of flavor compounds. *Journal of Agricultural and Food Chemistry*, *53*(19), 7518-7525. https://doi.org/10.1021/jf0507947.

Table 1. NGBLG, NPBLG, and FBLG binding parameters.

Parameters [a]	NGBLG	NPBLG	FBLG
m	12.5	9.5	20.5
K	3.1×10^{8}	5×10^{7}	5×10^{10}

[a] m = 1/n; n is the binding stoichiometry of NGBLG, NPBLG and FBLG to κ-car; K is the binding constant.

Figure captions

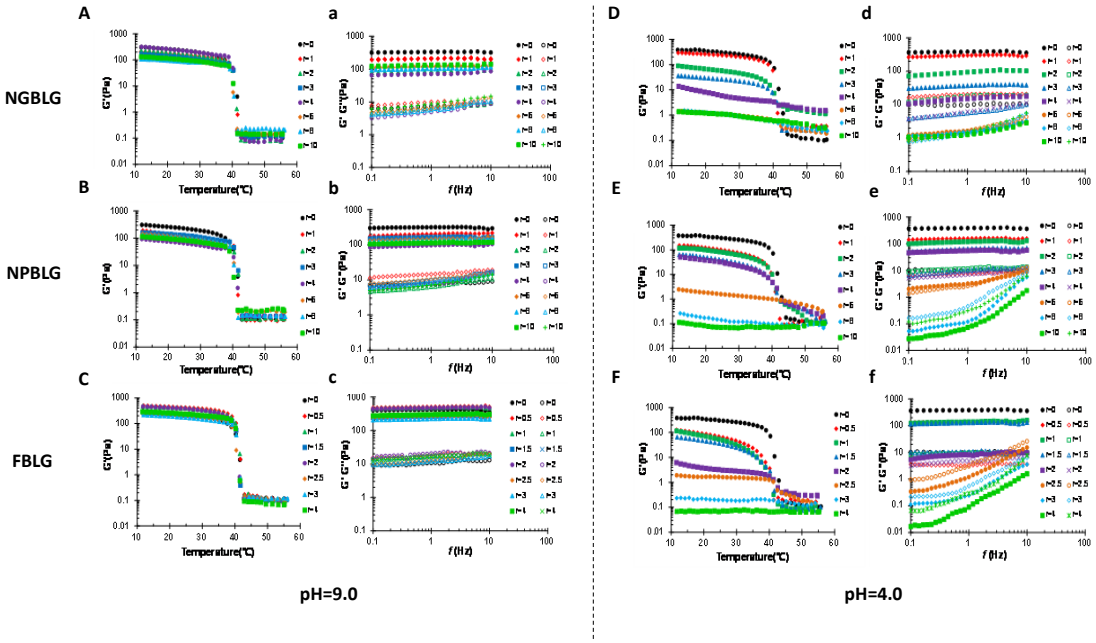

Fig. 1. Gelation profiles corresponding to mixtures of κ-car (0.15%, w/w) and NGBLG, NPBLG, or FBLG at different mixing ratios (r) in the presence of 50 mM KCl. The storage modulus (G′) versus temperature over the course of cooling is shown in A-C (pH 9.0) and D-F (at pH 4.0). The frequency sweep of storage (G′, closed symbol) and loss moduli (G″, open symbol) for these mixtures at 10 °C is shown in a-c (pH 9.0) and d-f (at pH 4.0).

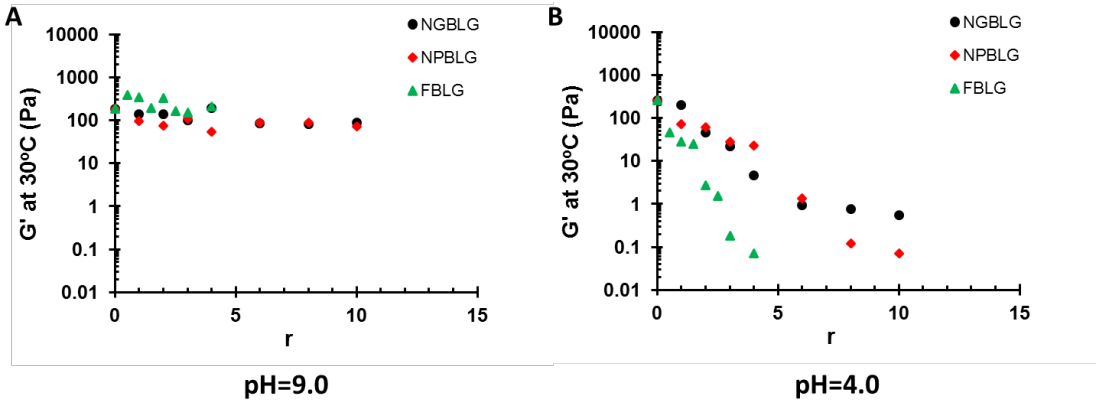

490

491 **Fig. 2.** The storage moduli G′ at 30°C and 1 Hz for κ-car (0.15%, w/w) at different NGBLG,

492 NPBLG, and FBLG/κ-car mixing ratios (r) at (A) pH 9.0 and (B) pH 4.0 in the presence of 50

493 mM KCl.

494

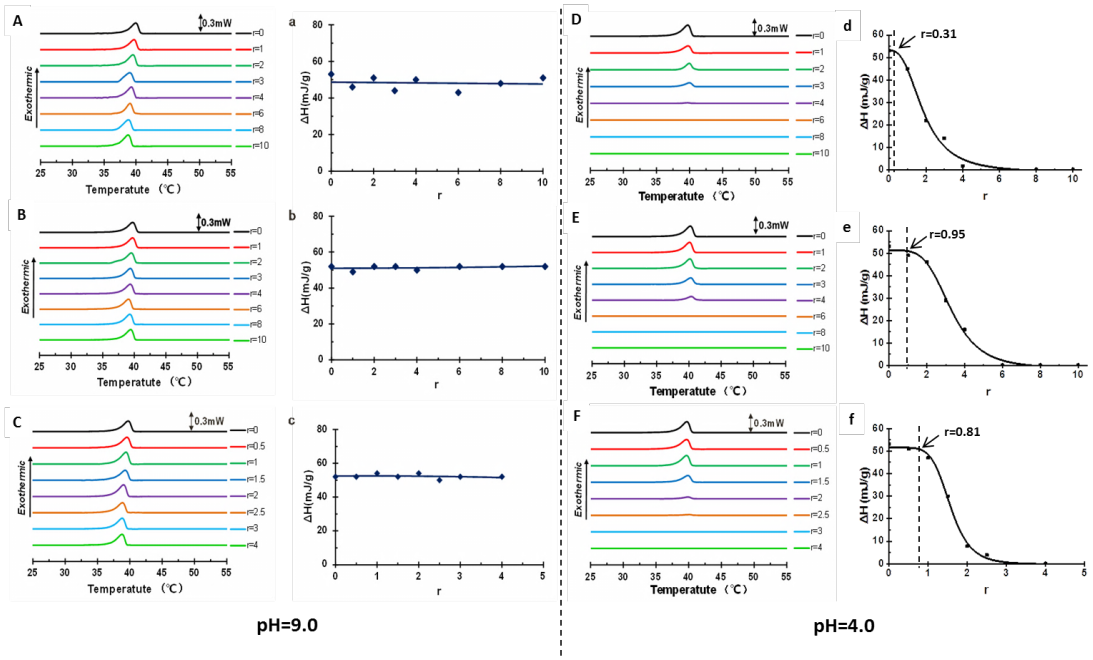

Fig. 3. DSC curves for κ-car (0.15%, w/w) in the presence of 50 mM KCl during cooling at a range of NGBLG/κ-car, NPBLG/κ-car, and FBLG/κ-car mixing ratios (r) at pH 9.0 (A-C) and pH 4.0 (D-F), respectively. The enthalpy change (ΔH) of the κ-car conformational transition at pH 9.0 (a-c) and pH 4.0 (d-f) as a function of r was also assessed. Corresponding mixing ratios for the indicated analyses are noted beside the DSC curves (A-F).

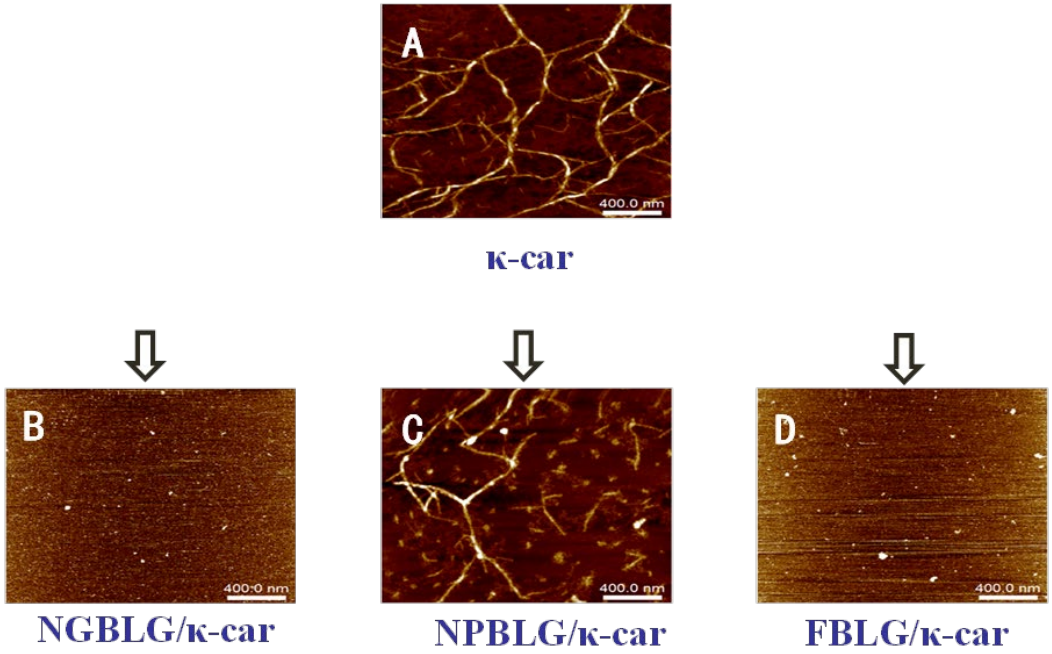

Fig. 4. AFM images the gel structure of κ-car (A) and mixtures thereof (B, C, D) at a fixed r = 3 and pH 4.0.

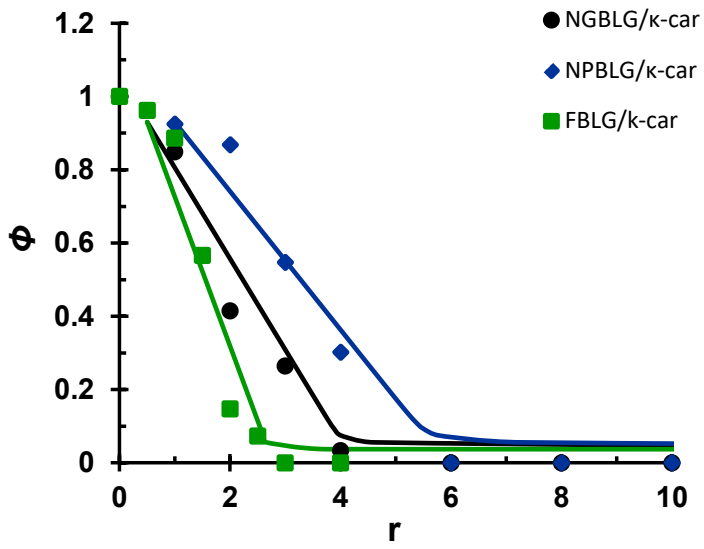

506

507 **Fig. 5.** Relative κ-car conformational transition (∅) as a function of NGBLG, NPBLG, and

508 FBLG/κ-car mixing ratios (r) at pH 4.0.

509

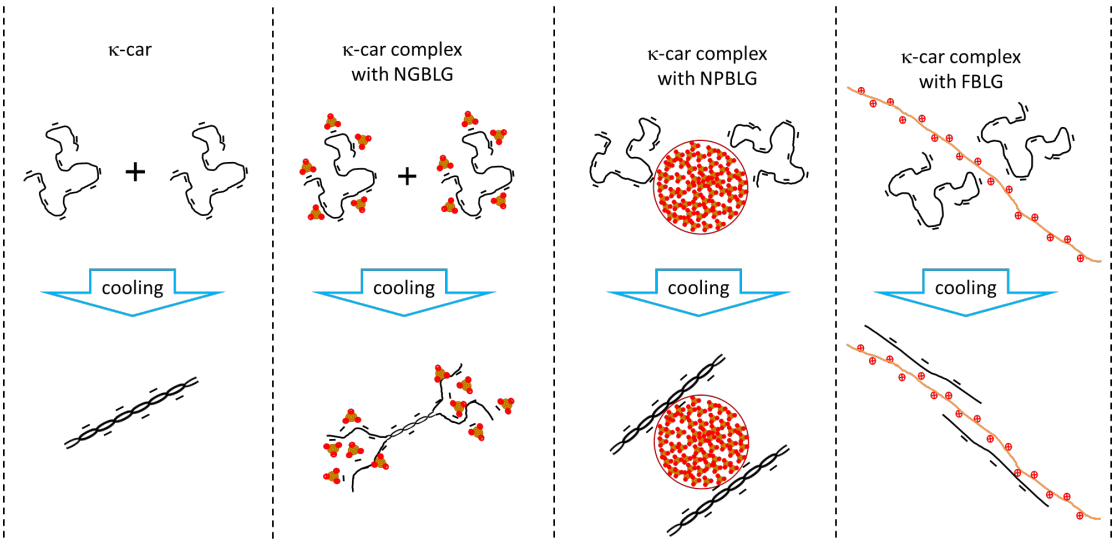

Fig. 6. A schematic overview of the impact of NGBLG, NPBLG, and FBLG electrostatic complexation on κ-car conformational transition upon cooling.